Newcastle University

ePrints

Al-Askery AJ, Tsimenidis C, Boussakta S, Chambers JA.
Performance Analysis of Coded Massive MIMO-OFDM Systems Using Effective Matrix Inversion.
***IEEE Transactions on Communications* 2017, (99)**
DOI link: https://doi.org/10.1109/TCOMM.2017.2749370

Copyright:

This work is licensed under a Creative Commons Attribution 3.0 License. For more information, see http://creativecommons.org/licenses/by/3.0/.

DOI link to article:

https://doi.org/10.1109/TCOMM.2017.2749370

Date deposited:

20/09/2017

This work is licensed under a Creative Commons Attribution 3.0 Unported License

Newcastle University ePrints - eprint.ncl.ac.uk

This article has been accepted for publication in a future issue of this journal, but has not been fully edited. Content may change prior to final publication. Citation information: DOI 10.1109/TCOMM.2017.2749370, IEEE Transactions on Communications

Performance Analysis of Coded Massive MIMO-OFDM Systems Using Effective Matrix Inversion

Ali J. Al-Askery, *Student Member, IEEE*, Charalampos C. Tsimenidis, *Senior Member, IEEE*, Said Boussakta, *Senior Member, IEEE*, and Jonathon A. Chambers, *Fellow, IEEE*

***Abstract*—In this paper, we derive the bit error rate (BER) and pairwise error probability (PEP) for massive multiple-input multiple-output orthogonal frequency-division multiplexing (MIMO-OFDM) systems for different M-ary modulations based upon the approximate noise distribution after channel equalization. The PEP is used to obtain the upper-bounds for convolutionally coded and turbo coded massive MIMO-OFDM systems for different code generators and receive antennas. In addition, complexity analysis of the log-likelihood ratio (LLR) values is performed using the approximate noise probability density function (PDF). The derived LLR computations can be time-consuming when the number of receive antennas is very large in massive MIMO-OFDM systems. Thus, a reduced complexity approximation is introduced using Newton's interpolation with different polynomial orders and the results are compared with the exact simulations. The Neumann large matrix approximation is used to design the receiver for a zero-forcing equalizer (ZFE) by reducing the number of operations required in calculating the channel matrix inverse. Simulations are used to demonstrate that the results obtained using the derived equations match closely the Monte-Carlo simulations.**

***Index Terms*—Massive MIMO-OFDM systems, performance analysis, convolutional codes, turbo codes**

I. Introduction

MASSIVE multiple-input multiple-output (MIMO) systems have recently attracted immense interest in the field of wireless communications due to their ability to increase data throughput and improve link quality [1]–[4]. Orthogonal frequency-division multiplexing (OFDM) is a multi-carrier technique with immunity to the channel's frequency selectivity, which can transmit data over large numbers of sub-carriers rather than a single carrier transmission [5], [6]. The combination of these two techniques in the form of a massive MIMO-OFDM system is a key technology for next generation wireless communication systems due to its improved performance compared to conventional MIMO systems [1], [7].

In addition, employing forward error correction (FEC) coding can further improve the performance of massive MIMO-OFDM systems due to the resulting frequency diversity and increased reliability of the transmitted data signals over K subcarriers and for N users [8]. Improvement in the bit error rate (BER) performance can reduce the number of receive antennas required to design coded massive MIMO-OFDM systems compared to uncoded systems [9]–[15].

To evaluate the performance of coded massive MIMO-OFDM systems time-consuming simulations are required. Thus, upper-bounds are of immense interest due to their ability to predict the performance of such a system. In [16]–[20], the upper-bounds of convolutional codes have been studied for the additive white Gaussian noise (AWGN) and for fading channels including different approximations. The performance of convolutionally coded MIMO systems for the MMSE detector has been derived in [21] using the moment generating function (MGF). In [22], a tight bound on a bit-interleaved space-time coded modulation (BI-STCM) scheme has been developed for MIMO systems with rate 1/2 convolutional code. Furthermore, the link-level capacity (LLC) and a tight bound have been derived in [23] for a MIMO-BICM system with a zero-forcing equalizer (ZFE) and a fast fading channel.

In [24], [25] the upper-bound of parallel concatenated codes assuming a uniform interleaver has been determined for turbo coded systems. The authors derived the upper-bound for both block and convolutional concatenated codes for an AWGN channel. In [26], an average bound has been proposed for the performance of turbo coded systems with correlated and uncorrelated Rayleigh fading channels. In [10], [27], the authors have proposed an upper-bound for the performance of the turbo coded MIMO system with correlated and uncorrelated Rayleigh, slow-fading channels, and the proposed bound approached the simulation results within 0.2-0.5 dB at a BER of 10^{-5}.

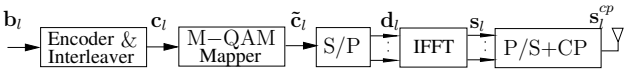

(a) l-th transmitter for the massive MIMO-OFDM systems.

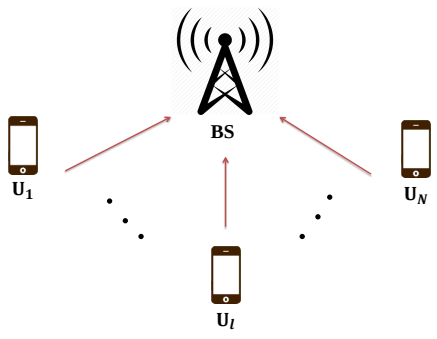

(b) Schematic diagram for the up-link transmission.

Fig. 1. N synchronous user transmitters for massive MIMO-OFDM systems.

This work is licensed under a Creative Commons Attribution 3.0 License. For more information, see http://creativecommons.org/licenses/by/3.0/.

This article has been accepted for publication in a future issue of this journal, but has not been fully edited. Content may change prior to final publication. Citation information: DOI 10.1109/TCOMM.2017.2749370, IEEE Transactions on Communications

In this paper, we focus on two significant technical differences between conventional MIMO-OFDM and massive MIMO-OFDM systems, which can be summarized in the following points:

- The massive number of receiving antennas at the base station, i.e. when $N_r \geqslant 10N$, has justified the exploitation of the diagonally dominant property of the Gram matrix. This assumption has reduced the complexity of evaluating the ZFE, and hence, the calculation of the noise probability density function (PDF).
- Having massive number of antennas at the base station has made it possible to use the central limit theorem (CLT) to approximate the distribution of the random variable by a Gaussian distribution [28], [29]. This property is used in this paper as part of proving the independence between the two random variables $\zeta_{l,k}$ and $\lambda^{\nu}_{l,k}$ that are the denominator and the numerator of (14).

To the best of our knowledge, no significant results have been presented in previous research works for the upper-bound performance of coded massive MIMO-OFDM systems. Our contributions can be summarized as follows:

- Based on the Neumann matrix inversion method, we derive an approximate PDF for the approximate noise after the ZFE.
- We derive the bit error rate (BER) for uncoded massive MIMO-OFDM systems with M-QAM modulation for frequency-selective, Rayleigh fading channels using the ZFE.
- We derive the pairwise error probability (PEP) for massive MIMO-OFDM systems.
- This PEP is subsequently used to evaluate the upper-bounds of the convolutionally coded and turbo coded systems.
- We estimate the complexity required in using the LLR equations based on the approximate noise PDF, and a reduced complexity based approximation is introduced for these LLRs using the Newton polynomial interpolation.

The rest of this paper is organized as follows. The system model is presented in Section II, and a brief introduction to the Neumann inversion method with the approximate noise PDF is illustrated in Section III. The BER is derived in Section IV for different modulation schemes, whereas the derivation of the PEP and the upper-bounds for coded MIMO-OFDM systems are presented in Section V for both convolutional and turbo coded systems. The complexity analysis employing the proposed approximation for the derived LLRs using the Newton interpolation is introduced in Section VI. Numerical results are discussed in Section VII, and conclusions are drawn in Section VIII.

Notation Matrices and vectors are denoted by upper-case and lower-case boldface characters, respectively. The Hermitian transpose of a matrix $\mathbf{A}$ and its pseudo-inverse are denoted by $\mathbf{A}^H$ and $\mathbf{A}^\dagger$, respectively. $\Gamma(a)$ and $\Gamma(a,b)$ are the complete and the incomplete gamma functions of the variables a and b. Finally, σ_w^2 and σ_H^2 are the noise and the channel variances, respectively. The subscripts l and n are used as indices for the l-th uplink user and the n-th receive antennas.

II. System Model

In this paper, an uplink coded multi-user (MU) massive MIMO-OFDM system is considered with $N_r \times N$ antennas as in Figs. 1 and 2 with $N_r >> N$. The terms N and N_r are used here to denote the number of users and the number of receive antennas, respectively. Each user has one transmit antenna and their transmissions are assumed to be synchronous, i.e. all users are transmitting and receiving their data at the same time. First, the binary data stream for each user, $\mathbf{b}_l$, is generated and encoded to produce the codewords, $\hat{\mathbf{c}}_l$, which are randomly interleaved, $\mathbf{c}_l = \Pi(\hat{\mathbf{c}}_l)$ and modulated using an M-ary quadrature amplitude modulation (M-QAM), i.e. $\tilde{\mathbf{c}}_l = C(\mathbf{c}_l)$, where, Π and C represent the interleaving and constellation mapping operations, respectively.

After the modulation, the OFDM waveform for each user is individually constructed, i.e. $\mathbf{s}_l = \mathbf{F}^H \mathbf{d}_l$, where $\mathbf{d}_l$ is the modulated vector for the l-th user, $\mathbf{F} \in \mathbb{C}^{K\times K}$ is the discrete Fourier transform (DFT) matrix with $f_{m,n} = \frac{1}{\sqrt{K}} e^{-j2\pi \frac{mn}{K}}$, $\forall m,n = 1,2,\cdots,K-1$, and K is the block length of the inverse DFT (IDFT) used in the OFDM modulators. To avoid multipath-induced, inter-block interference (IBI) and inter-symbol interference (ISI), a cyclic prefix (CP) is inserted at the start of each block to cover the excess delay spread of the channel, that is

$$\mathbf{s}_l^{cp} = \left[s_{K-K_{cp}}, \ldots, s_{K-1}, s_0, \ldots, s_{K-1}\right]^T, \tag{1}$$

where K_{cp} is the length of the cyclic prefix which is selected to be longer than the channel delay spread. The transmitted signals propagate through time-flat, frequency-selective fading channels and are received in the presence of complex zero-mean additive white Gaussian noise (AWGN) of variance σ_w^2. This work assumes that the channel state information (CSI) is perfectly available at the receiver side and has been estimated using the methods proposed in [30]–[34]. After OFDM demodulation, involving CP removal and the DFT at each of the N_r antennas, the received signal vector, $\mathbf{r}_k \in \mathbb{C}^{N_r\times 1}$, for the k-th subcarrier can be written as

$$\mathbf{r}_k = \mathbf{H}_k \mathbf{d}_k + \mathbf{w}_k, \tag{2}$$

where $\mathbf{H}_k \in \mathbb{C}^{N_r\times N}$ is the channel matrix in the frequency domain and $\mathbf{w}_k \in \mathbb{C}^{N_r\times 1}$ is the DFT of the time-domain AWGN samples. To detect the transmitted information symbols, a ZFE can be utilized as follows

$$\tilde{\mathbf{d}}_k = \mathbf{H}_k^\dagger \mathbf{r}_k = \mathbf{d}_k + \mathbf{H}_k^\dagger \mathbf{w}_k, \tag{3}$$

where $\mathbf{H_k}^\dagger$ is the ZFE vector that can be obtained using the pseudo-inverse of $\mathbf{H_k}$ defined as

$$\mathbf{H}_k^\dagger = \mathbf{G}_k^{-1}\mathbf{H}_k^H, \tag{4}$$

and $\mathbf{G}_k = \mathbf{H}_k^H\mathbf{H}_k$ is the symmetric Gram matrix of the channel. A closer examination of the noise term in (3) reveals that the ZFE operation affects the distribution of the noise, and the Gaussian assumption can not be used to describe its properties as shown in (3) since it is a ratio distribution with Gaussian at the numerator and Rayleigh at the denominator. Therefore, in

This work is licensed under a Creative Commons Attribution 3.0 License. For more information, see http://creativecommons.org/licenses/by/3.0/.

This article has been accepted for publication in a future issue of this journal, but has not been fully edited. Content may change prior to final publication. Citation information: DOI 10.1109/TCOMM.2017.2749370, IEEE Transactions on Communications

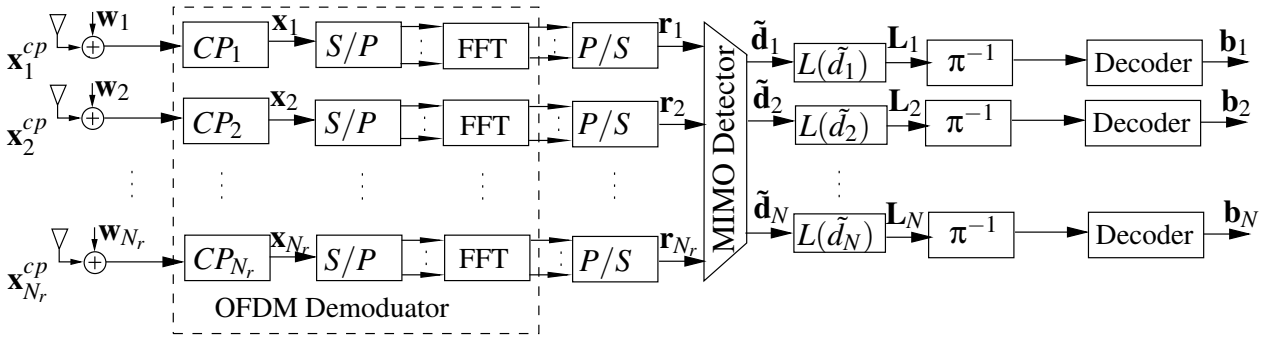

Fig. 2. Receiver for Massive MIMO-OFDM systems with Forward Error Correcting Coding (FECC).

order to improve the performance of detection, a more accurate noise model is needed. In the next section, we proceed with the derivation of the PDF for the approximate noise. It is also worth noting that the DFT and IDFT operations are performed in practice using their corresponding fast Fourier transform implementations.

III. APPROXIMATE NOISE PDF

For massive matrices, the Gram matrix becomes diagonally dominant [2], [35]. This property can be exploited to compute the Gram matrix using the Neumann series approximation method to reduce the complexity in calculating the Moore-Penrose pseudo-inverse. In (4), $\mathbf{G}_k$ is involved in calculating the ZFE and can be decomposed into two matrices, i.e. $\mathbf{G}_d$, which is composed only of diagonal elements, and $\mathbf{G}_e = \mathbf{G}_k - \mathbf{G}_d$, containing only the off-diagonal elements of $\mathbf{G}_k$. The Neumann matrix inverse for $\mathbf{G}_k$ can be given as [35]

$$\mathbf{G}_k^{-1} = \sum_{n=0}^{L} \left(-\mathbf{G}_d^{-1}\mathbf{G}_e\right)^n \mathbf{G}_d^{-1}. \tag{5}$$

The complexity involved in calculating this inverse will depend on L, which controls the number of terms in the summation of (5). For massive MIMO systems, that is $N_r \geqslant 10N$, an accurate approximation of $\mathbf{G}_k$ can be obtained for $L = 0$ [35]. In this case, the Gram matrix inverse will be reduced to a diagonal matrix inversion, which will simplify the procedure required to find the PDF of $\mathbf{G}_k^{-1}$ as illustrated in the next section. As stated previously [36], the Neumann series approximation can be used to efficiently rewrite (4) in the following form,

$$\mathbf{H}_k^{\dagger} = \mathbf{G}_d^{-1}\mathbf{H}_k^H. \tag{6}$$

Therefore, the noise term in (3) at the output of the ZFE detector becomes

$$\tilde{\mathbf{w}}_k = \mathbf{G}_d^{-1}\mathbf{H}_k^H\mathbf{w}_k. \tag{7}$$

For the l-th transmit user, the PDF of $\mathbf{G}_d$ is a Chi-square distribution with $2N_r$ degrees of freedom and can be given as [37], [36]

$$p(\zeta_{l,k}) = \frac{|\zeta_{l,k}|^{N_r-1}}{(2\sigma_H^2)^{N_r}\Gamma(N_r)} \exp\left(-\frac{|\zeta_{l,k}|}{2\sigma_H^2}\right), \tag{8}$$

where, $\zeta_{l,k} = \sum_{n=1}^{N_r} |H_{n,l}(k)|^2$ for $l = 1, 2, \ldots, N$ and σ_H^2 is the average variance of $H_{n,l}(k)$. It is worth noting that the mean of $\zeta_{l,k}$ is $\mu_\zeta = 2N_r\sigma_H^2$ and the variance is $\sigma_\zeta^2 = 4N_r\sigma_H^4$. The mean squared error (MSE) method which can be calculated as $MSE = \sum_k (p(\zeta_{l,k}) - \hat{p}_{l,k})^2/K$, is used here to calculate the error resulting from the difference between the empirical and theoretical PDF, where $\hat{p}_{l,k}$ is the simulation of the PDF for $\zeta_{l,k}$. In addition, the Kolmogorov-Smirnov (KS) goodness-of-fit test [38] is applied at 5% significance level with the null hypothesis that the two vectors exhibit the same distribution. Fig. 3 a) shows the empirical and theoretical PDF, i.e. (8), for a system with $N = 10$ and $N_r = 200$ at an SNR of -10 dB demonstrating a very close agreement. In this case, the computed value of the MSE is 9.9176×10^{-9} and the KS test decision is 0 implying that we can not reject the null hypothesis.

Furthermore, each element, $\lambda_{l,k}$ of the vector $\boldsymbol{\lambda}_k = \mathbf{H}_k^H\mathbf{w}_k$ can be given as

$$\lambda_{l,k} = \sum_{n=1}^{N_r} H_{n,l}^*(k) w_{n,k}, \tag{9}$$

therefore, its inphase (I) and quadrature (Q) components exhibit the following forms, respectively

$$\lambda_{l,k}^I = \sum_{n=1}^{N_r} H_{n,l}^I(k) w_{n,k}^I + H_{n,l}^Q(k) w_{n,k}^Q, \tag{10}$$

and

$$\lambda_{l,k}^Q = \sum_{n=1}^{N_r} H_{n,l}^Q(k) w_{n,k}^I - H_{n,l}^I(k) w_{n,k}^Q. \tag{11}$$

As can be seen, $\lambda_{l,k}^I$, $\lambda_{l,k}^Q$ are the result of a sum of products for $2N_r$ independent Gaussian variables. It was shown in [19] that their distribution can be given as

$$p(\lambda_{l,k}^\nu) = \frac{\exp(\frac{-|\lambda_{l,k}^\nu|}{\sigma_H\sigma_w})}{\Gamma(N_r)\ \sigma_H\sigma_w} \times \sum_{n=1}^{N_r} \frac{(N_r+n-2)!}{(N_r-n)!\ 2^{N_r+n-1}\ \Gamma(n)} \left(\frac{\left|\lambda_{l,k}^\nu\right|}{\sigma_H\sigma_w}\right)^{N_r-n}, \tag{12}$$

This work is licensed under a Creative Commons Attribution 3.0 License. For more information, see http://creativecommons.org/licenses/by/3.0/.

This article has been accepted for publication in a future issue of this journal, but has not been fully edited. Content may change prior to final publication. Citation information: DOI 10.1109/TCOMM.2017.2749370, IEEE Transactions on Communications

where $\nu = \{I, Q\}$. By taking the statistical expectation of (10) and (11), it is straightforward to show that the mean value of $\lambda^{\nu}_{l,k}$ is zero, i.e. $\mu_{\lambda^{\nu}_{l,k}} = 0$, and its variance can be theoretically computed as

$$\begin{aligned}\sigma^2_{\lambda^{\nu}_{l,k}} &= \int_{-\infty}^{\infty} (\lambda^{\nu}_{l,k})^2 \; p(\lambda^{\nu}_{l,k}) d\lambda^{\nu}_{l,k} \\ &= \sum_{n=1}^{N_r} \frac{\Gamma(N_r+n-1)}{\Gamma(N_r)\Gamma(N_r-n+1)\Gamma(n)2^{(Nr+n-2)}} \\ &\times \frac{\int_0^{\infty} (\lambda^{\nu}_{l,k})^{N_r-n+2} \exp(\frac{-\lambda^{\nu}_{l,k}}{\sigma_H \sigma_w}) d\lambda^{\nu}_{l,k}}{(\sigma_H \sigma_w)^{N_r-n+1}} \\ &= \sum_{n=1}^{N_r} \frac{\Gamma(N_r-n+3)\Gamma(N_r+n-1)(\sigma_H \; \sigma_w)^2}{\Gamma(N_r)\Gamma(N_r-n+1)\Gamma(n)2^{(Nr+n-2)}} \end{aligned} \quad (13)$$

The empirical PDF of $\lambda^{\nu}_{l,k}$ and its theoretical PDF given in (12) demonstrate a very close agreement as shown in Fig. 3 b). The computed value of MSE is 8.874×10^{-10} and the KS test decision is 0 implying that the null hypothesis can not be rejected.

Next, the l-th random variable for the approximate noise after the ZFE can be written based on (7) as

$$\alpha^{\nu}_{l,k} = \frac{\lambda^{\nu}_{l,k}}{\zeta_{l,k}}. \quad (14)$$

The two random variables, $\lambda^{\nu}_{l,k}$ and $\zeta_{l,k}$, are assumed to be statistically independent random variables based on the proof that is provided in Appendix B. Therefore, the joint PDF of $\zeta_{l,k}$ and $\lambda^{\nu}_{l,k}$ can be written as follows

$$p(\lambda^{\nu}_{l,k}, \zeta_{l,k}) = p(\zeta_{l,k}) p(\lambda^{\nu}_{l,k}), \quad (15)$$

By integrating this joint PDF with respect to $\zeta_{l,k}$ and substituting $\lambda^{\nu}_{l,k} = \alpha^{\nu}_{l,k}\zeta_{l,k}$, the noise PDF can be obtained as

$$p(\alpha^{\nu}_{l,k}) = \sum_{n=1}^{N_r} \frac{(N_r+n-2)!(2N_r-n)!(\frac{\sigma_w}{2\sigma_H})^{N_r}}{2^{N_r+n-1}\Gamma^2(N_r)(N_r-n)!\Gamma(n)} \times \frac{\left|\alpha^{\nu}_{l,k}\right|^{N_r-n}}{\left(\left|\alpha^{\nu}_{l,k}\right| + \frac{\sigma_w}{2\sigma_H}\right)^{2N_r-n+1}}. \quad (16)$$

The mean value of this PDF is zero and its variance is given as

$$\sigma^2_{\alpha^{\nu}_{l,k}} = \sum_{n=1}^{N_r} \frac{\Gamma(N_r-n+3)\Gamma(N_r+n-1)\Gamma(N_r-2)\left(\frac{\sigma_w}{\sigma_H}\right)^2}{\Gamma^2(N_r)\Gamma(N_r-n+1)\Gamma(n)2^{(Nr+n)}}. \quad (17)$$

The details of these derivations can be found in Appendix A. To verify the accuracy of this PDF, a comparison between the histogram plot of the actual noise PDF and this equation is given in Fig. 3 c). A close inspection of the figure reveals that the empirical PDF of $\alpha^{\nu}_{l,k}$ and its theoretical PDF given in (16) are closely matched. The computed MSE is 2.076×10^{-5}, while the KS test decision is 0, thus, verifying the validity of the null hypothesis.

Using the PDF in (16) describing the noise characteristics after the ZFE, we proceed to derive the BER, the PEP, and the upper-bounds for the performance of convolutionally coded and turbo coded massive MIMO-OFDM systems.

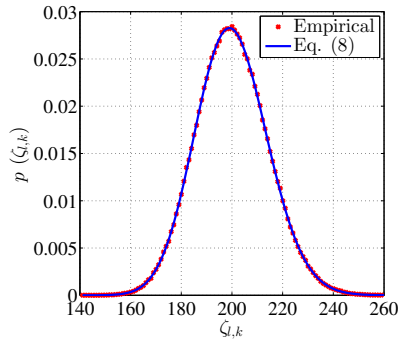

(a) PDF plot for $p(\zeta_{l,k})$

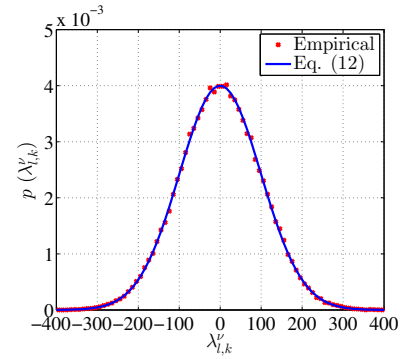

(b) PDF plot for $p(\lambda^{\nu}_{l,k})$

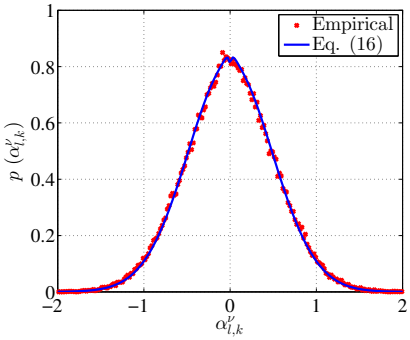

(c) PDF plot for $p(\alpha^{\nu}_{l,k})$

Fig. 3. Histogram plot of the equalised noise versus the derived PDFs .

IV. Bit Error Rate (BER)

In this section, we start with the derivation of the BER of 4-QAM scheme and then extend the derivations to include higher QAM constellations.

1) 4-QAM scheme: Deriving the BER for the 4-QAM scheme requires the computation of the following integration for the real and imaginary parts [37], [39]

$$P^{\nu}_{e} = \int_0^{\infty} p(\alpha^{\nu}_{l,k} + 1) \; d\alpha^{\nu}_{l,k}. \quad (18)$$

The solution for this integration is obtained by substituting (51) and (52), as found in Appendix A, in (16) and integrating

This work is licensed under a Creative Commons Attribution 3.0 License. For more information, see http://creativecommons.org/licenses/by/3.0/.

This article has been accepted for publication in a future issue of this journal, but has not been fully edited. Content may change prior to final publication. Citation information: DOI 10.1109/TCOMM.2017.2749370, IEEE Transactions on Communications

$$P_e^{\nu}=\int_0^{\infty}\int_0^{\infty}\sum_{n=1}^{N_r}\frac{(N_r+n-2)!\,|\zeta_{l,k}|^{2N_r-n}\exp\left(-\frac{|\zeta_{l,k}|}{2\sigma_H^2}\right)\exp\left(\frac{-\left|(\alpha_{l,k}^{\nu}+1)\zeta_{l,k}\right|}{\sigma_H\sigma_w}\right)\left(\left|\alpha_{l,k}^{\nu}+1\right|\right)^{N_r-n}}{(2\sigma_H^2)^{N_r}(\sigma_H\sigma_w)^{N_r-n+1}(N_r-n)!\;2^{N_r+n-1}\;\Gamma(n)\Gamma^2(N_r)}d\alpha_{l,k}^{\nu}d\zeta_{l,k}, \tag{19}$$

(19) in two steps with respect to $\alpha_{l,k}^{\nu}$ and $\zeta_{l,k}$. First, we integrate with respect to $\alpha_{l,k}^{\nu}$ to obtain I_1, i.e.

$$I_1^{\nu}=\int_0^{\infty}\left(\left|\alpha_{l,k}^{\nu}+1\right|\right)^{N_r-n}\exp\left(\frac{-\left|(\alpha_{l,k}^{\nu}+1)\zeta_{l,k}\right|}{\sigma_w\;\sigma_H}\right)d\alpha_{l,k}^{\nu}. \tag{20}$$

The solution for (20) is obtained using [40, Eq. (3.351.2)]

$$I_1^{\nu}=\frac{(N_r-n)!\exp(-\frac{|\zeta_{l,k}|}{\sigma_w\sigma_H})}{(\frac{|\zeta_{l,k}|}{\sigma_w\sigma_H})^{N_r-n+1}}\sum_{m=0}^{N_r-n}\frac{(\frac{|\zeta_{l,k}|}{\sigma_w\sigma_H})^m}{m!}. \tag{21}$$

Similarly, integrating with respect to $\zeta_{l,k}$ results in

$$I_2^{\nu}=\int_0^{\infty}|\zeta_{l,k}|^{N_r+m-1}\exp\left(-|\zeta_{l,k}|\,\eta\right)d\zeta_{l,k}, \tag{22}$$

where $\eta=(\frac{\sigma_w+2\sigma_H}{2\sigma_H^2\sigma_w})$. Solving (22) using [40, Eq. (3.351.3)], we obtain I_2 as

$$I_2^{\nu}=\frac{\Gamma(N_r+m)}{\eta^{N_r+m}}. \tag{23}$$

Substituting I_1^{ν} and I_2^{ν} in (19), results in

$$P_e^{\nu}=\frac{(\frac{\sigma_w}{2\sigma_H})^{N_r}}{2^{N_r-1}\Gamma^2(N_r)}\times\sum_{n=1}^{N_r}\sum_{m=0}^{N_r-n}\frac{2^{-n}(N_r+n-2)!\Gamma(N_r+m)}{m!\;\Gamma(n)(1+\frac{\sigma_w}{2\sigma_H})^{N_r+m}}. \tag{24}$$

Now, the probability of correct decision for one symbol of the 4-QAM can be written as

$$P_c=(1-P_e^{\nu})^2=1-2P_e^{\nu}+(P_e^{\nu})^2, \tag{25}$$

and the symbol error rate (SER) can be written as

$$P_s^{4-QAM}=1-P_c\approx 2P_e^{\nu}. \tag{26}$$

After straightforward mathematical manipulations, the BER for the massive MIMO-OFDM systems with 4-QAM scheme can be written as

$$P_e^{4-QAM}=\frac{(\frac{\sigma_w}{2\sigma_H})^{N_r}}{2^{N_r-1}\Gamma^2(N_r)}\times\sum_{n=1}^{N_r}\sum_{m=0}^{N_r-n}\frac{2^{-n}(N_r+n-2)!\Gamma(N_r+m)}{m!\;\Gamma(n)(1+\frac{\sigma_w}{2\sigma_H})^{N_r+m}}. \tag{27}$$

2) 4-Pulse Amplitude Modulation (4-PAM) and 16-QAM modulation: The BER for higher QAM constellations can be determined using the relationship between the PAM and QAM schemes [37]

$$P_s^{M-QAM}=1-(1-P_s^{\sqrt{M}-PAM})^2, \tag{28}$$

$$P_e^{M-QAM}=\frac{P_s^{M-QAM}}{\log_2 M}, \tag{29}$$

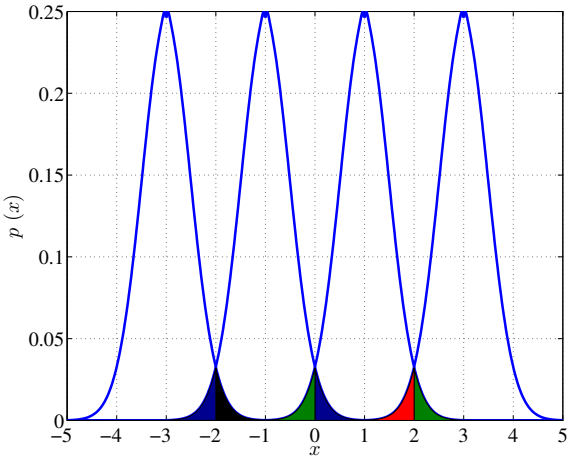

Fig. 4. Noise distribution in 4-PAM modulated massive MIMO-OFDM with $N=10$ and $N_r=100$.

where P_s^{M-QAM} and $P_s^{\sqrt{M}-PAM}$ denote the symbol error rate (SER) for the QAM and PAM modulations, respectively, and P_e^{M-QAM} is the BER for M-QAM. The SER for the 4-PAM can be derived by exploiting the noise distribution in Fig. 4. For practical SNR ranges, only 6 error events need to be considered that are distributed within 4 equiprobable noise PDFs. Due to symmetry, the SER can be obtained by considering a single error event. The error probability generated by the noise PDF $p(|\alpha_{l,k}^{\nu}+3|)$ can be calculated as

$$P_{s_1}=\int_{-2}^{\infty}p(\left|\alpha_{l,k}^{\nu}+3\right|)d\alpha_{l,k}. \tag{30}$$

The result of this integration is similar to (18), hence, the SER for the 4-PAM modulation can be written as

$$P_s^{4-PAM}=\frac{6}{4}P_{s_1}=\frac{3(\frac{\sigma_w}{2\sigma_H})^{N_r}}{2^{N_r}\Gamma^2(N_r)}\times\sum_{n=1}^{N_r}\sum_{m=0}^{N_r-n}\frac{2^{-n}(N_r+n-2)!\;\Gamma(N_r+m)}{m!\;\Gamma(n)\;(1+\frac{\sigma_w}{2\sigma_H})^{N_r+m}}. \tag{31}$$

Subsequently, the SER and the BER for 16-QAM can be determined by substituting (31) into (28) and the outcome in (29). In the next section, the pairwise error probability (PEP), the upper-bound of the convolutionally coded and turbo coded massive MIMO-OFDM systems will be calculated based on the noise distribution in (16).

V. Bounds for Coded Massive MIMO-OFDM Systems

In this section, the PEP between any two different code words will be derived based on the noise distribution after

This work is licensed under a Creative Commons Attribution 3.0 License. For more information, see http://creativecommons.org/licenses/by/3.0/.

This article has been accepted for publication in a future issue of this journal, but has not been fully edited. Content may change prior to final publication. Citation information: DOI 10.1109/TCOMM.2017.2749370, IEEE Transactions on Communications

the ZFE shown in (16). Then, an upper-bound for the convolutionally coded massive MIMO-OFDM systems is obtained by combining this PEP with the error weights listed in [17], [18]. In addition, an average-bound for turbo coded massive MIMO-OFDM systems is derived using the method introduced in [24].

A. Pairwise Error Probability

The probability of incorrectly decoding the code word $\mathbf{d}_2$ instead of the code word $\mathbf{d}_1$ is known as the pairwise error probability (PEP). Based on (3) and the noise distribution of (16), the PEP can be written as [41]

$$\begin{aligned} P_{\mathbf{d}_1\to\mathbf{d}_2} &= p(||\tilde{\mathbf{d}}-\mathbf{d}_1||^2 > ||\tilde{\mathbf{d}}-\mathbf{d}_2||^2)\ , \\ &= p(||\mathbf{d}_1+\tilde{\mathbf{w}}-\mathbf{d}_1||^2 > ||\mathbf{d}_1+\tilde{\mathbf{w}}-\mathbf{d}_2||^2)\ , \\ &= p(\tilde{\mathbf{w}} > \frac{||\mathbf{d}_2-\mathbf{d}_1||}{2})\ , \end{aligned} \tag{32}$$

where $P_{\mathbf{d}_1\to\mathbf{d}_2}$ is the PEP. Next, we substitute $||\mathbf{d}_2-\mathbf{d}_1|| = 2\sqrt{E_c d}$, where d is the Hamming distance of the code, and E_c is the coded bit energy. Thus, the PEP can be written as [42]

$$P_{\mathbf{d}_1\to\mathbf{d}_2} = \int_{\sqrt{E_c d}}^{\infty} p(\alpha_{l,k}^{\nu}) d\alpha_{l,k}^{\nu}\ , \tag{33}$$

The result of this integration can be given as

$$P_{\mathbf{d}_1\to\mathbf{d}_2} = \frac{(\frac{\sigma_w}{2\sigma_H})^{N_r}}{2^{N_r-1}\Gamma^2(N_r)}\times \sum_{n=1}^{N_r}\sum_{m=0}^{N_r-n} \frac{2^{-n}(N_r+n-2)!\Gamma(N_r+m)}{m!\ \Gamma(n)(1+\frac{\sigma_w}{2\sigma_H\sqrt{E_c d}})^{N_r+m}(E_c d)^{\frac{N_r}{2}}}. \tag{34}$$

B. Upper-Bounds for convolutionally coded massive MIMO-OFDM systems

According to [17], [18], the upper-bound for convolutionally coded systems has been shown to have the form

$$P_b < \sum_{d=d_{free}}^{\infty} c_d P_{\mathbf{d}_1\to\mathbf{d}_2}(d), \tag{35}$$

where d is the Hamming distance, d_{free} is the minimum Hamming distance that is used to calculate the error correction capability of that code, $P_{\mathbf{d}_1\to\mathbf{d}_2}(d)$ is the pairwise error probability and c_d is the sum of error events for each d. In this work, the pairwise error probability for the massive MIMO-OFDM systems is obtained in (34). Thus, the upper-bound equation for the coded massive MIMO-OFDM systems can be written as

$$P_b < \sum_{d=d_{free}}^{\infty} \frac{c_d(\frac{\sigma_w}{2\sigma_H})^{N_r}}{2^{N_r-1}\Gamma^2(N_r)}\times \sum_{n=1}^{N_r}\sum_{m=0}^{N_r-n} \frac{2^{-n}(N_r+n-2)!\Gamma(N_r+m)}{m!\ \Gamma(n)(1+\frac{\sigma_w}{2\sigma_H\sqrt{E_c d}})^{N_r+m}(E_c d)^{\frac{N_r}{2}}}. \tag{36}$$

In Appendix C, the number of error events c_d are tabulated for two selected codes with octal generator polynomials $(23,35)_8$ and $(247,371)_8$ for code rate $1/2$, [17], [18].

C. Asymptotic upper-bounds for turbo coded massive MIMO-OFDM systems

The excellent performance of turbo codes in wireless communication systems has attracted much attention. However, deriving the bounds for these codes is more complicated than for convolutional codes as they consist typically of two parallel concatenated convolutional codes (PCCC) separated by an interleaver. Serial concatenation is common too. An average-bound has been derived using the input-redundancy weight enumerating function (IRWEF) for the combination of two convolutional codes involved in the construction of the turbo code. First, the conditional weight enumerating function (CWEF) is derived from the transfer function of each code, then an average CWEF ($A_{\iota j,\delta\varrho}^{C_p}(\omega,Z)$) is calculated using [24]

$$A_{\iota j,\delta\varrho}^{C_p}(\omega,Z) = \frac{A_{\iota\delta}^{C_1}(\omega,Z)A_{j\varrho}^{C_2}(\omega,Z)}{\binom{N_\iota}{\omega}}, \tag{37}$$

where $A_{\iota\delta}^{C_1}(\omega,Z)$ and $A_{j\varrho}^{C_2}(\omega,Z)$ are the CWEFs of the first and the second convolutional codes, denoted C_1 and C_2, respectively; ω is the Hamming weight of the input information, N_ι is the interleaver length, and finally, $\binom{N_\iota}{\omega}$ is the binomial distribution of the parameters N_ι and ω. Hence, the IRWEF can be obtained using the average CWEF as follows

$$A^C(W,Z) = \sum_{\iota j,\delta\varrho} W^{\iota j,\delta\varrho}\ A_{\iota j,\delta\varrho}^{Cp}(\omega,Z). \tag{38}$$

The average bound of the turbo coded system has the form

$$P_b \approx \sum_d D_d P_{\mathbf{d}_1\to\mathbf{d}_2}(d), \tag{39}$$

where, $P_{\mathbf{d}_1\to\mathbf{d}_2}(d)$ is given in (34) and D_d factors are tabulated in [24] for different interleaver lengths and can be calculated using

$$D_d = \sum_{f+\omega=d} \frac{\omega}{N_\iota} A_{\omega,f}, \tag{40}$$

where f is the Hamming weight of the parity bits. The symbol $A_{w,f}$ represents the number of code words with Hamming distance $d=w+f$, that is the sum of the Hamming distances for the information w and reliability f bits. The $A_{w,f}$ values are the coefficients of the IRWEF that is calculated in (38).

VI. Complexity calculations and log-likelihood ratio (LLR) approximations

The output of the ZFE in (3) is utilized to calculate the LLR equations required for soft decoding, which are given as

$$L(\tilde{\mathbf{d}}_{l,k}^I) = \ln\left(\frac{p(\alpha_{l,k}^I|_{\tilde{d}_{l,k}^I=1})}{p(\alpha_{l,k}^I|_{\tilde{d}_{l,k}^I=-1})}\right), \tag{41}$$

$$L(\tilde{\mathbf{d}}_{l,k}^Q) = \ln\left(\frac{p(\alpha_{l,k}^Q|_{\tilde{d}_{l,k}^Q=1})}{p(\alpha_{l,k}^Q|_{\tilde{d}_{l,k}^Q=-1})}\right). \tag{42}$$

where the subscripts I and Q denote the in-phase and quadrature parts of complex-valued signals, respectively.

This work is licensed under a Creative Commons Attribution 3.0 License. For more information, see http://creativecommons.org/licenses/by/3.0/.

This article has been accepted for publication in a future issue of this journal, but has not been fully edited. Content may change prior to final publication. Citation information: DOI 10.1109/TCOMM.2017.2749370, IEEE Transactions on Communications

When the number of receive antennas is relatively high in massive MIMO systems, the LLR calculations using the PDF of (16) will exhibit higher complexity compared to other approximated PDF approaches such as the Gaussian distribution. However, as will be demonstrated in Section VIII, the utilization of the proposed LLRs based on the newly derived PDF results in a significant performance improvement.

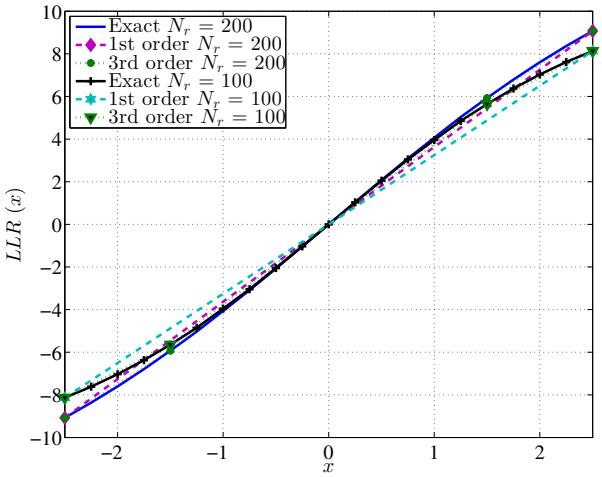

Fig. 5. Plot of exact and approximate LLR for $(N = 10, N_r = 100, 200)$.

On the other hand, a reduced complexity approach can be used to simplify the soft bit calculations evaluated based on this PDF by approximating the LLR values, without affecting the system performance significantly. We use polynomial interpolation to approximate the LLR equations by a low order polynomial [43], [44]. For 4-QAM, the real and imaginary parts of the received symbols after ZFE are scaled in the range -2.5 to 2.5 with 4 points distributed as $\{-2.5, -1.25, 1.25, 2.5\}$. Subsequently, the evaluation procedure starts by calculating the Newton table that will be used to determine the polynomial coefficients. By applying the regression procedure, the equivalent LLR equation for the selected example can be written as

$$L(x) = \sum_{\rho=0}^{N_x} a_\rho x^\rho, \tag{43}$$

where values of a_ρ parameters are listed in Table I and N_x is the polynomial order. This equation will reduce the complexity

TABLE I
a_ρ PARAMETERS FOR LLR APPROXIMATION

N_r	a_0	a_1	a_2	a_3
100 3rd order	0	4.02502	0	-0.1275
100 1st order	0	3.2524	0	0
150 3rd order	0	4.1269	0	-0.1027
150 1st order	0	3.485	0	0
200 3rd order	0	4.27	0	-0.0842
200 1st order	0	3.4441	0	0

of the exact LLR as shown in Table II, where N_x is selected to obtain 1st and 3rd order polynomials. The plot of the actual LLR equation versus (43) is demonstrated in Fig. 5 for both approximated LLRs.

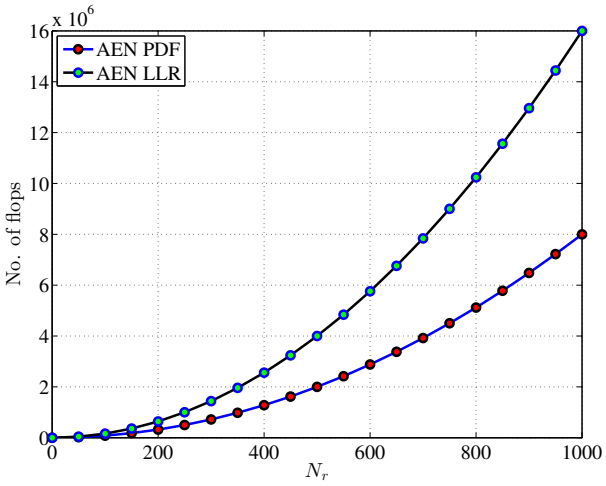

Fig. 6. Number of flops required to calculate the LLR using the approximate PDF.

The $gaxpy$ operation denotes a matrix-vector multiplication plus a vector addition of the form $\mathbf{y} = \mathbf{y} + \mathbf{Ax}$, where $\mathbf{y}$ and $\mathbf{x}$ are vectors and $\mathbf{A}$ is a matrix [45]. It is used here to determine the number of operations required in calculating (16), (41), (42) and (43) as shown in Table II. The number of operations required to calculate the approximate noise (AN) PDF depends mainly on N_r, whereas using the Gaussian PDF in calculating the LLRs is limited to one multiplication which is equivalent to the proposed approximation using the Newton interpolation.

TABLE II
OPERATIONS REQUIRED

Equation	Div.	Add.	Sub.	Mul.
Eq. (16)	$2N_r + 2$	$2N_r$	$6N_r + 1$	$8{N_r}^2 + 3N_r - 2$
LLR AN	$4N_r + 1$	$4N_r$	$12N_r$	$16{N_r}^2 - 2N_r$
LLR Gaussian	0	0	0	1
LLR App. 1st	0	0	0	1
LLR App. 3rd	0	0	1	4

The floating point operation (FLOP) counts of the $gaxpy$ approach weighs higher the most nested operations rather than the exact complexity [45]. Based on that, Fig. 6 shows the effect of increasing N_r on the total complexity, assuming that the number of flops required to calculate (16) is $O(8N_r^2)$, and for the exact LLR is $O(16N_r^2)$.

The obtained results will be thoroughly discussed in the next section.

VII. NUMERICAL RESULTS

Numerical results are presented in this section to evaluate the performance of the derived formulas. For simulation purposes, the number of receive antennas are selected in the range, $N_r \in [100, 200]$ and the number of users are in the range, $N \in [4, 10]$, respectively. The $SNR = \frac{E_b N}{2\sigma_w^2 R}$, where R is the coding rate, the FFT length is 1024, the CP $= 128$ and the Universal

This work is licensed under a Creative Commons Attribution 3.0 License. For more information, see http://creativecommons.org/licenses/by/3.0/.

This article has been accepted for publication in a future issue of this journal, but has not been fully edited. Content may change prior to final publication. Citation information: DOI 10.1109/TCOMM.2017.2749370, IEEE Transactions on Communications

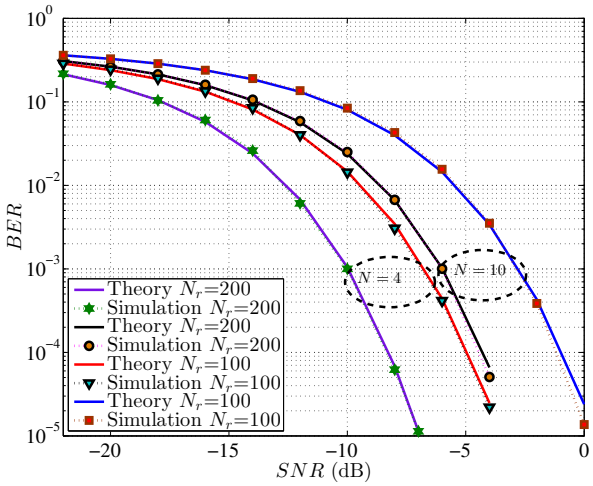

Fig. 7. BER performance for massive MIMO-OFDM system with $N = 4, 10$ and $N_r = 100, 200$ for 4-QAM.

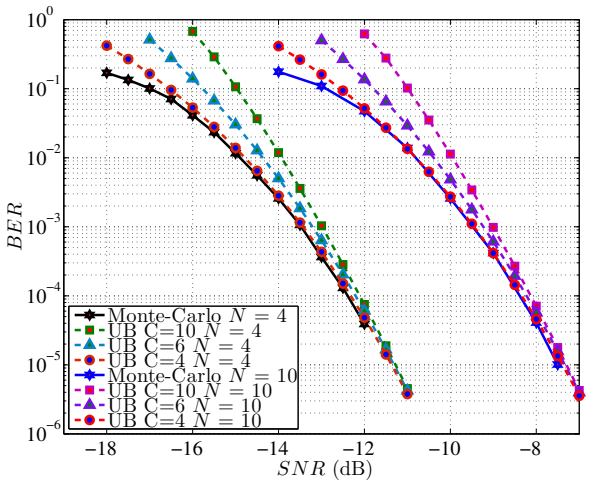

Fig. 9. Upper-bound for convolutionally coded massive MIMO-OFDM system with $(23, 35)_8$ and $N = 4, 10$, $N_r = 200$. C represents the index for c_d.

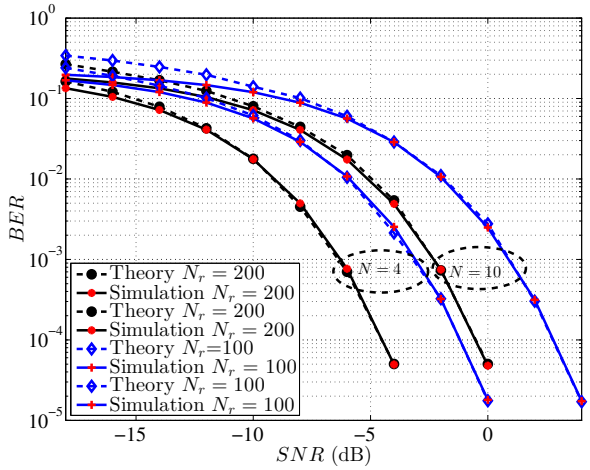

Fig. 8. BER performance for massive MIMO-OFDM system with $N = 4, 10$ and $N_r = 100, 200$ for 16-QAM.

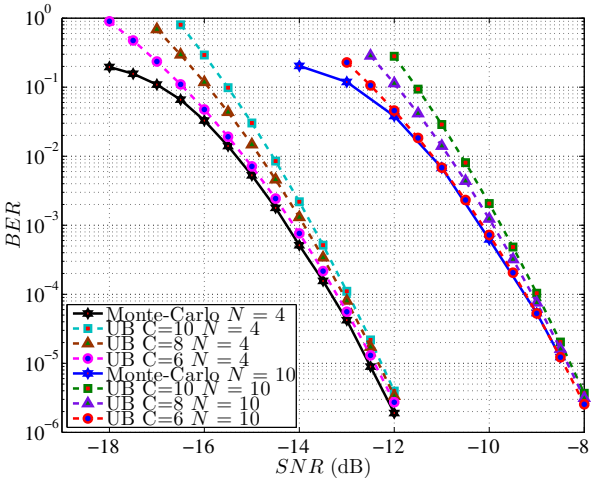

Fig. 10. Upper-bound for convolutionally coded massive MIMO-OFDM system with $(247, 371)_8$ and $N = 4, 10$, $N_r = 200$. C represents the index for c_d.

Mobile Telecommunications Service (UMTS) interleaver size is selected as 1024 to maintain good performance with reduced simulation time. The transmitted signals propagate through time-flat, frequency-selective Rayleigh fading channels with 6 multipath arrivals and a delay spread of maximum 85 samples and are received in the presence of complex zero-mean AWGN of variance σ_w^2.

In Section IV, we used the PDF of (16) to derive the BER equation of the massive MIMO-OFDM system with different modulation types. To verify the BER for 4-QAM and 16-QAM using (27) and (29), respectively, the theoretical performance of the massive MIMO-OFDM system is compared with Monte-Carlo simulations using $N = 4, 10$ and $N_r = 100, 200$ and the obtained performances are illustrated in Figs. 7 and 8 both of which show close match between theory and simulations.

In Section V-B, an upper-bound to the convolutionally coded massive MIMO-OFDM systems has been derived by adding the effect of Hamming distance to the PEP derived in Section V-A and using the error weights derived from the transfer function of the desired convolutional code [17], [18]. The upper-bound in Figs. 9 and 10 is controlled by the index of c_d in Table III which is written as C. For example, when the index of c_d is higher than 10 a divergence in upper-bound performance was noticed that tends to be a straight line bounding the simulation. However, reducing this index will result in a tighter bound that depends on the constraint length of the desired convolutional code. For instance the $(23, 35)_8$ code has an index of 4, while the $(247, 371)_8$ code has an index of 6. In addition, we have estimated the asymptotic upper-bound of the turbo coded system using the CWEF method described in [24], [25]. We have used the earlier derived PEP along with the D_m factors derived from the IRWEF for the $(5, 7)_8$ PCCC. The results shown in Figs. 11 and 12 demonstrate the bound for the turbo coded systems

This work is licensed under a Creative Commons Attribution 3.0 License. For more information, see http://creativecommons.org/licenses/by/3.0/.

This article has been accepted for publication in a future issue of this journal, but has not been fully edited. Content may change prior to final publication. Citation information: DOI 10.1109/TCOMM.2017.2749370, IEEE Transactions on Communications

with $N_r = 200$ and $N = 4, 10$, respectively. The asymptotic upper-bound in these figures shows close match to the highest iteration of the turbo coded massive MIMO-OFDM system with less than 0.15 dB difference in BER performance when $N = 10$ and less than 0.4 dB when $N = 4$. It is also observed that the performance bounds are a function of the number of iterations, as can be seen in the cases of 4 and 50 iterations in both figures. As a result, this asymptotic upper-bound provides a meaningful bound to the performance of turbo coded systems when the BER is below 10^{-3}, while it is less useful below this value.

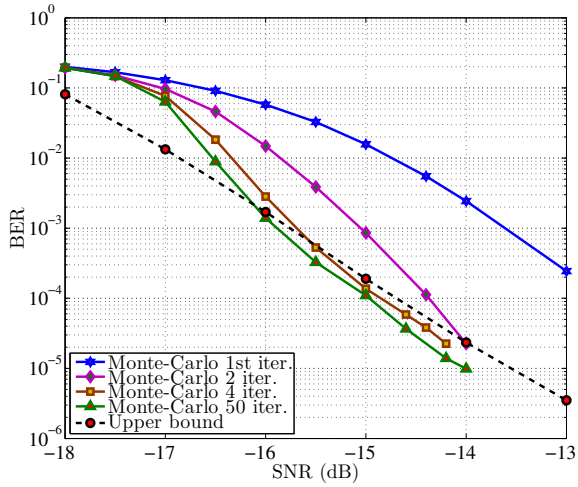

Fig. 11. Asymptotic upper-bound turbo coded massive MIMO-OFDM system with $(5, 7)_8$ Generator and $N = 4$, $N_r = 200$ and for different number of iterations.

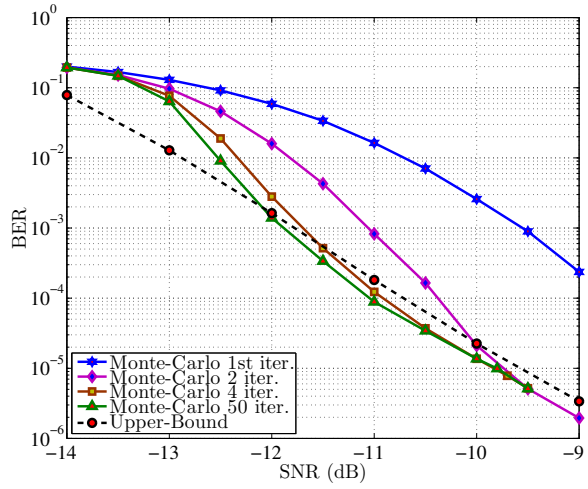

Fig. 12. Asymptotic upper-bound turbo coded massive MIMO-OFDM system with $(5, 7)_8$ Generator and $N = 10$, $N_r = 200$ and for different number of iterations.

Furthermore, using the LLR equations based on the newly derived PDF has improved the BER performance of the turbo coded massive MIMO-OFDM system by 0.8 dB at 10^{-4} BER. To reduce the cost of using this LLR, we have used the Newton's interpolation method to rewrite this equation

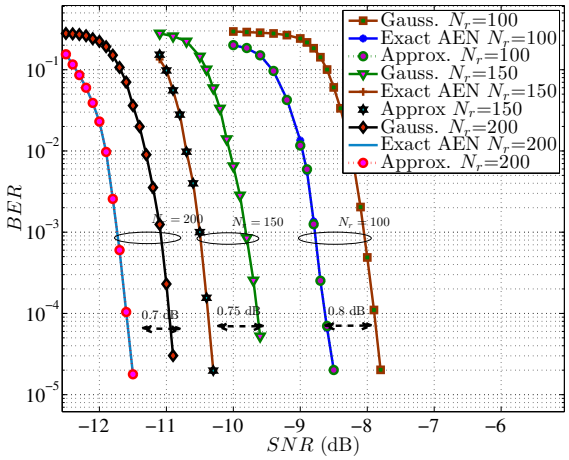

Fig. 13. Simulation of the turbo coded massive MIMO-OFDM system with $(561, 753)_8$, and $N = 10$ and $N_r = 100, 150, 200$.

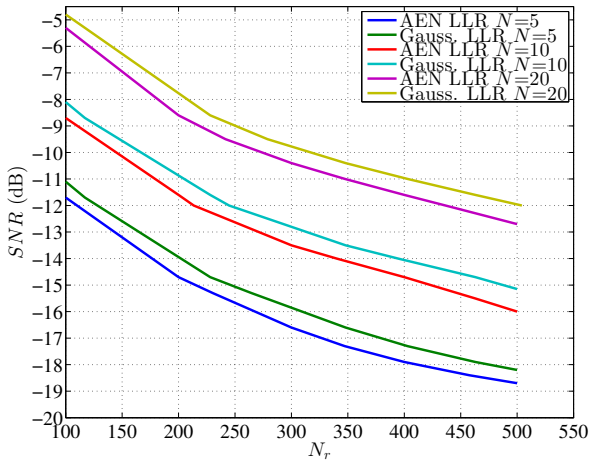

Fig. 14. Comparing the number of required received antennas in Gaussian PDF based LLR and the exact LLR at different transmit and receive antennas.

as a linear polynomial of different orders. According to the results shown in Fig. 13, the first order approximation has successfully matched the BER performance of the derived LLR and reduced the complexity to one multiplication as shown in Table II.

Finally, Fig. 14 demonstrates the reduction in the number of required receive antennas when using the exact LLRs compared to LLRs derived based on the Gaussian assumption as a function of the SNR. Closer observation of the figure shows that to obtain a BER performance of 10^{-5} at an SNR of -14.6 dB, we need $N_r = 400$ receive antennas for the exact LLR computations, while the Gaussian based LLRs require $N_r = 470$ antennas to achieve the same performance at $N = 10$ users. Thus, using error correction with exact LLR computations, a reduction of 70 antenna elements and their corresponding RF chains can be achieved. Furthermore, increasing the number of users from 5 to 10, to 20 results in a reduction of 2.4 and 3.5 dB for the approximate PDF approach respectively. In contrast, for the Gaussian based PDF

This work is licensed under a Creative Commons Attribution 3.0 License. For more information, see http://creativecommons.org/licenses/by/3.0/.

This article has been accepted for publication in a future issue of this journal, but has not been fully edited. Content may change prior to final publication. Citation information: DOI 10.1109/TCOMM.2017.2749370, IEEE Transactions on Communications

the degradation is in both cases 3 dB.

VIII. Conclusion

In this paper, we have derived the BER for massive MIMO-OFDM systems by deriving and using the approximate noise PDF after the ZFE. The derived BER has been verified using the Monte-Carlo simulations for different number of users and receive antennas and the results have shown close match between the theory and numerical evaluation. Then, the PEP has been derived in Section V-A and used to obtain an upper-bound for convolutionally encoded massive MIMO-OFDM systems. The results have bounded the performance for different error weight values and indices, and the upper-bound performance became very tight for the two selected codes. In addition, the turbo coded system is bounded within 0.15 dB of the Monte-Carlo simulations by using the derived PEP and the D_m terms given for the $(5,7)_8$ PCCC using 4-QAM scheme. Furthermore, calculating the LLR using the PDF of (16) improved the performance compared to the Gaussian assumption resulting in a reduction of the required number of receive antennas by 70 at an SNR of -14.6 dB. However, this new PDF increased the computational complexity of LLR calculations, thus, increasing the overall receiver complexity. To reduce this complexity and to maintain good performance, we have suggested an equivalent LLR equation with a low complexity design using Newton polynomial interpolation. The performance of this approximated LLR equation showed a close match to the exact LLR with negligible complexity.

Acknowledgement

This work was supported by the EPSRC under project EP/N004299/1, Cooperative Backhaul Aided Next-Generation Digital Subscriber Loops. The authors would like to thank the Research Council for this funding. No new data were created during this study.

Appendix A
Deriving the noise PDF

A. Deriving the Gram matrix distribution

The Gram matrix $\mathbf{G}_k$ of the MIMO channel $\mathbf{H_k}$ can be written as

$$\begin{aligned}\mathbf{G_k} &= E\{\mathbf{H_k}^H\mathbf{H_k}\}\ , \\ &= \begin{bmatrix} \sum_{n=1}^{N_r}|H_{n,1}(k)|^2 & & \mathbf{0} \\ & \ddots & \\ \mathbf{0} & & \sum_{n=1}^{N_r}|H_{n,N}(k)|^2 \end{bmatrix}. \end{aligned} \quad (44)$$

Each diagonal element has the following form

$$\zeta_{l,k} = \sum_{n=1}^{N_r}|H_{n,l}(k)|^2 = \zeta_{1,l}(k)+\zeta_{2,l}(k)+\cdots+\zeta_{N_r,l}(k), \quad (45)$$

where the elements $\zeta_{n,l}(k) = (H^I_{n,l}(k))^2 + (H^Q_{n,l}(k))^2$ are real-valued random variables with 2 degrees of freedom. The characteristic function for these random variables can be written in the form [37]

$$\psi_{\zeta_{k,i}}(w) = \left(\frac{1}{1-j2\sigma_H^2 w}\right), \quad (46)$$

The distribution for the summation in (45) can be represented as N_r convolutions of $\zeta_{n,l}(k)$, which means N_r multiplications in the frequency domain. The characteristic function and the resulting PDF of (45) can be written as

$$\psi_{\zeta_{l,k}}(w) = \left(\frac{1}{1-j2\sigma_H^2 w}\right)^{N_r}, \quad (47)$$

$$p(\zeta_{l,k}) = \frac{|\zeta_{l,k}|^{N_r-1}\ \exp\left(-\frac{|\zeta_{l,k}|}{2\sigma_H^2}\right)}{(2\sigma_H^2)^{N_r}\Gamma(N_r)}. \quad (48)$$

B. Deriving the Noise PDF

The real and imaginary parts of the noise term in (7) have symmetric PDFs, and hence, we will derive a general equation to represent both parts. First, the noise equation at the output of the MIMO detector can be written as

$$\begin{bmatrix} \frac{1}{\zeta_{1,k}} & 0 & 0 \\ 0 & \frac{1}{\zeta_{l,k}} & 0 \\ \vdots & \cdots & \vdots \\ 0 & 0 & \frac{1}{\zeta_{N,k}} \end{bmatrix} \begin{bmatrix} \lambda^\nu_{1,k} \\ \lambda^\nu_{l,k} \\ \vdots \\ \lambda^\nu_{N,k} \end{bmatrix} = \begin{bmatrix} \frac{\lambda^\nu_{1,k}}{\zeta_{1,k}} \\ \frac{\lambda^\nu_{l,k}}{\zeta_{l,k}} \\ \vdots \\ \frac{\lambda^\nu_{N,k}}{\zeta_{N,k}} \end{bmatrix} = \begin{bmatrix} \alpha^\nu_{1,k} \\ \alpha^\nu_{l,k} \\ \vdots \\ \alpha^\nu_{N,k} \end{bmatrix}. \quad (49)$$

The joint probability of $\lambda^\nu_{l,k}$ and $\zeta_{l,k}$ can then be written as [36]

$$p(\lambda^\nu_{l,k},\zeta_{l,k}) = p(\lambda^\nu_{l,k})p(\zeta_{l,k}) = \frac{|\zeta_{l,k}|^{N_r-1}\ \exp\left(-\frac{|\zeta_{l,k}|}{2\sigma_H^2}\right)}{(2\sigma_H^2)^{N_r}\Gamma(N_r)} \times \sum_{n=1}^{N_r} \frac{\exp(\frac{-|\lambda^\nu_{l,k}|}{\sigma_H\sigma_w})\Gamma(N_r+n-1)\left|\lambda^\nu_{l,k}\right|^{N_r-n}}{(N_r-n)!\ 2^{N_r+n-1}\Gamma(n)\sigma_H{\sigma_w}^{N_r-n}\Gamma(N_r)}, \quad (50)$$

and the substitution of $\lambda^\nu_{l,k} = \zeta_{l,k}\alpha^\nu_{l,k}$ in this equation will result in

$$p(\alpha^\nu_{l,k}\zeta_{l,k},\zeta_{l,k}) = \sum_{n=1}^{N_r} A_n \exp\left(-\beta\left|\zeta_{l,k}\right|\right)\left|\zeta_{l,k}\right|^{2N_r-n-1}, \quad (51)$$

where A_n and β are equal to

$$A_n = \frac{\left|\alpha^\nu_{l,k}\right|^{N_r-n}(N_r+n-2)!(\sigma_H\sigma_w)^{n-N_r-1}}{\Gamma^2(N_r)(2\sigma_H^2)^{N_r}(N_r-n)!\ 2^{N_r+n-1}\Gamma(n)},$$

$$\beta = \frac{\sigma_w + 2\sigma_H\left|\alpha^\nu_{l,k}\right|}{2\sigma_w\sigma_H}.$$

This work is licensed under a Creative Commons Attribution 3.0 License. For more information, see http://creativecommons.org/licenses/by/3.0/.

This article has been accepted for publication in a future issue of this journal, but has not been fully edited. Content may change prior to final publication. Citation information: DOI 10.1109/TCOMM.2017.2749370, IEEE Transactions on Communications

Now, to find the noise PDF, we must integrate this equation w.r.t $\zeta_{l,k}$ as [36], [46]

$$p(\alpha_{l,k}^{\nu}) = \int_{-\infty}^{\infty} |\zeta_{l,k}|\, p(\alpha_{l,k}^{\nu}\zeta_{l,k}, \zeta_{l,k}) d\zeta_{l,k} \tag{52}$$

$$p(\alpha_{l,k}^{\nu}) = \sum_{n=1}^{N_r} \frac{(N_r+n-2)!(2N_r-n)!(\frac{\sigma_w}{2\sigma_H})^{N_r}}{2^{N_r+n-1}\Gamma^2(N_r)(N_r-n)!\Gamma(n)} \times \frac{\left|\alpha_{l,k}^{\nu}\right|^{N_r-n}}{(\left|\alpha_{l,k}^{\nu}\right| + \frac{\sigma_w}{2\sigma_H})^{2N_r-n+1}}. \tag{53}$$

APPENDIX B
VERIFICATION OF INDEPENDENCE

To verify that the two random variables $\lambda_{l,k}^{\nu}$ and $\zeta_{l,k}$ can be assumed to be independent, the following points will be considered.

First, the central limit theorem (CLT) states that, suppose $X_1, X_2, \ldots X_n$ are i.i.d. random variables with mean μ and variance $\sigma^2 < \infty$ and defining

$$S_n = \frac{1}{\sigma\sqrt{n}} \sum_{i=1}^{n} (X_i - \mu) \ . \tag{54}$$

Then, for large n, S_n can approximately be considered to be normally distributed with mean μ and variance $\frac{\sigma^2}{n}$ [28], [29]. To be more specific, as long as the value $n > 10$, as stated in [47] the distribution of S_n approaches the normal distribution.

As such, since $N_r \geq 100$, the PDF of the real and imaginary parts of $\lambda_{l,k} = \sum_{n=1}^{N_r} H_{n,l}^{*}(k) w_{n,k}$, can be written in the form of a normal distribution with $N(0, \sigma_{\lambda}^2)$ as

$$p(\lambda_{l,k}^{\nu}) = \frac{1}{\sqrt{2\pi\sigma_{\lambda}^2}} \exp(-\frac{{\lambda_{l,k}^{\nu}}^2}{2\sigma_{\lambda}^2}). \tag{55}$$

Similarly, the PDF of $\zeta_{l,k} = \sum_{n=1}^{N_r} |H_{n,l}(k)|^2$ for large N_r, can be written as $N(\mu_{\zeta}, \sigma_{\zeta}^2)$

$$p(\zeta_{l,k}) = \frac{1}{\sqrt{2\pi\sigma_{\zeta}^2}} \exp(-\frac{(\zeta_{l,k}-\mu_{\zeta})^2}{2\sigma_{\zeta}^2}), \tag{56}$$

where the theoretical values of $\sigma_{\lambda}^2, \mu_{\zeta}, \sigma_{\zeta}^2$ are calculated in Section III. Next, based on this large N_r assumption, the two Gaussian random variables will be independent if their covariance is zero. Thus, we will proceed to calculate the covariance of $\zeta_{l,k}$ and $\lambda_{l,k}^{\nu}$, $c_{\zeta\lambda}$, to verify they are independent random variables. $c_{\zeta\lambda}$ is computed as

$$\begin{aligned} c_{\zeta\lambda} &= E\{(\zeta_{l,k} - \mu_{\zeta})\lambda_{l,k}\} \ , \\ &= E\{\zeta_{l,k}\lambda_{l,k}\} - \mu_{\zeta} E\{\lambda_{l,k}\} \ . \end{aligned} \tag{57}$$

Since $E\{\lambda_{l,k}\} = 0$, the covariance of (57) can be written as

$$\begin{aligned} c_{\zeta\lambda} &= E\{\zeta_{l,k}\lambda_{l,k}\} \ , \\ &= E\Big\{ \sum_{n=1}^{N_r} |H_{n,l}(k)|^2 \sum_{m=1}^{N_r} H_{m,l}^{*}(k) w_{m,k} \Big\} \ . \end{aligned} \tag{58}$$

By expanding the inner sum

$$\begin{aligned} c_{\zeta\lambda} = E\{ &\sum_{n=1}^{N_r} |H_{n,l}(k)|^2 H_{1,l}(k)^* w_{1,k} + \sum_{n=1}^{N_r} |H_{n,l}(k)|^2 \times \\ &H_{2,l}(k)^* w_{2,k} + \ldots + \sum_{n=1}^{N_r} |H_{n,l}(k)|^2 H_{N_r,l}(k)^* w_{N_r,k} \} \ , \end{aligned} \tag{59}$$

and then expanding the outer sum, we obtain

$$\begin{aligned} c_{\zeta\lambda} = E\{ &|H_{1,l}(k)|^2 H_{1,l}(k)^* w_{1,k} + |H_{1,l}(k)|^2 H_{2,l}(k)^* w_{2,k} \\ &+ \ldots + |H_{1,l}(k)|^2 H_{N_r,l}(k)^* w_{N_r,k} + |H_{2,l}(k)|^2 \times \\ &H_{1,l}(k)^* w_{1,k} + |H_{2,l}(k)|^2 H_{2,l}(k)^* w_{2,k} + \ldots + \\ &|H_{2,l}(k)|^2 H_{N_r,l}(k)^* w_{N_r,k} + \ldots + \\ &|H_{N_r,l}(k)|^2 H_{N_r,l}(k)^* w_{N_r,k} \} \ . \end{aligned} \tag{60}$$

Since the channel parameters and the AWGN are independently distributed, we can write (60) as

$$\begin{aligned} c_{\zeta\lambda} = &E\{|H_{1,l}(k)|^2 H_{1,l}(k)^*\} E\{w_{1,k}\} + \\ &E\{|H_{1,l}(k)|^2 H_{2,l}(k)^*\} E\{w_{2,k}\} + \ldots + \\ &E\{|H_{1,l}(k)|^2 H_{N_r,l}(k)^*\} E\{w_{N_r,k}\} + \ldots + \\ &E\{|H_{N_r,l}(k)|^2 H_{N_r,l}(k)^*\} E\{w_{N_r,k}\} \ . \end{aligned} \tag{61}$$

The AWGN has zero mean which makes the term $E\{w_{m,k}\} = 0$, and the covariance $c_{\zeta\lambda} = 0$. As a result, we have two independent Gaussian distributed random variables [29], and their joint probability can be written as shown in (15).

APPENDIX C
ERROR WEIGHTS

TABLE III
RATE 1/2 ERROR WEIGHTS FOR SELECTED CODES [17], [18]

Generators	$(23,35)_8$	$(247,371)_8$
K, d_{free}	5,7	8,10
c_{d_f}	4	2
c_{d_f+1}	12	22
c_{d_f+2}	20	60
c_{d_f+3}	72	148
c_{d_f+4}	225	340
c_{d_f+5}	500	1008
c_{d_f+6}	1324	2642
c_{d_f+7}	3680	6748
c_{d_f+8}	8967	18312
c_{d_f+9}	22270	48478
c_{d_f+10}	57403	126364
c_{d_f+11}	142234	320062
c_{d_f+12}	348830	821350
c_{d_f+13}	867106	2102864
c_{d_f+14}	2134239	5335734
c_{d_f+15}	5205290	13549068
c_{d_f+16}	12724352	34254388
c_{d_f+17}	31022962	86441848
c_{d_f+18}	75250693	217480314
c_{d_f+19}	182320864	545858054

This work is licensed under a Creative Commons Attribution 3.0 License. For more information, see http://creativecommons.org/licenses/by/3.0/.

This article has been accepted for publication in a future issue of this journal, but has not been fully edited. Content may change prior to final publication. Citation information: DOI 10.1109/TCOMM.2017.2749370, IEEE Transactions on Communications

REFERENCES

[1] J. G. Andrews, S. Buzzi, W. Choi, S. V. Hanly, A. Lozano, A. C. K. Soong, and J. C. Zhang, "What will 5G be?" *IEEE J. Sel. Areas Commun.*, vol. 32, no. 6, pp. 1065–1082, 2014.

[2] M. Wu, B. Yin, G. Wang, C. Dick, J. Cavallaro, and C. Studer, "Large-scale MIMO detection for 3GPP LTE: algorithms and FPGA implementations," *IEEE J. Sel. Topics Signal Process.*, vol. 8, no. 5, pp. 916–929, Oct 2014.

[3] S. Yang and L. Hanzo, "Fifty years of MIMO detection: the road to large-scale MIMOs," *IEEE Commun. Surveys Tuts.*, vol. 17, no. 4, pp. 1941–1988, 2015.

[4] A. Elghariani and M. Zoltowski, "Low complexity detection algorithms in large-scale MIMO systems," *IEEE Trans. Wireless Commun.*, vol. 15, no. 3, pp. 1689–1702, 2016.

[5] S. Younis, A. Al-Dweik, C. C. Tsimenidis, B. S. Sharif, and A. Hazmi, "Robust early-late gate system for symbol timing recovery in MIMO-OFDM systems," in *Proc. IEEE 7th Int. Conf. Wireless Mobile Comput. Netw. Commun. (WiMob)*, 2011, pp. 416–421.

[6] M. I. Asseri, S. Y. L. Goff, C. C. Tsimenidis, and B. S. Sharif, "Efficient recovery of dSLM in MIMO-OFDM without side information," in *Proc. 5th Adv. Int. Conf. Telecommun. (AICT)*., 2009, pp. 158–162.

[7] E. Baar, "Multiple-input multiple-output OFDM with index modulation," *IEEE Signal Process. Lett.*, vol. 22, no. 12, pp. 2259–2263, 2015.

[8] C. Roth, S. Belfanti, C. Benkeser, and Q. Huang, "Efficient parallel turbo-decoding for high-throughput wireless systems," *IEEE Trans. Circuits Syst. I*, vol. 61, no. 6, pp. 1824–1835, 2014.

[9] Y. L. Ueng, C. J. Yeh, and C. L. W. M. C. Lin, "Iterative detection and decoding for the near-capacity performance of turbo coded MIMO schemes," in *Proc. IEEE 18th Int. Symp. Personal Indoor Mobile Radio Commun.*, 2007, pp. 1–5.

[10] N. Mysore and J. Bajcsy, "Union bound based performance evaluation of turbo-coded uplink MIMO systems," in *Proc. IEEE Military Commun. Conf. (MILCOM)*, 2005, pp. 2837–2843 Vol. 5.

[11] L. Boher, M. Helard, and R. Rabineau, "Turbo-coded MIMO iterative receiver with bit per bit interference cancellation for M-QAM gray mapping modulation," in *Proc. IEEE 65th Veh. Technol. Conf. (VTC)*, 2007, pp. 2394–2398.

[12] Y. L. Ueng and Y. M. Chen, "A turbo coded MIMO scheme for noncoherent fast-fading channels," in *Proc. IEEE 66th Veh. Technol. Conf. (VTC)*, 2008, pp. 1350–1354.

[13] P. Shang, S. Kim, and K. Choi, "Soft ZF MIMO detection for turbo codes," in *Proc. IEEE 6th Int. Conf. Wireless Mobile Comput. Netw. Commun. (WiMob)*, 2010, pp. 116–120.

[14] P. Shang, S. Kim, and K. Choi, "Soft MMSE receiver for turbo coded MIMO system," in *Proc. IEEE 7th Int. Conf. Wireless Mobile Comput. Netw. Commun. (WiMob)*, 2011, pp. 471–475.

[15] K. J. Kim, T. Reid, and R. A. Iltis, "Iterative soft-QRD-M for turbo coded MIMO-OFDM systems," *IEEE Trans. Commun.*, vol. 56, no. 7, pp. 1043–1046, 2008.

[16] A. Viterbi, "Convolutional codes and their performance in communication systems," *IEEE Trans. Commun. Technol.*, vol. 19, no. 5, pp. 751–772, October 1971.

[17] J. Conan, "The weight spectra of some short low-rate convolutional codes," *IEEE Trans. Commun.*, vol. 32, no. 9, pp. 1050–1053, 1984.

[18] P. Frenger, P. Orten, and T. Ottosson, "Convolutional codes with optimum distance spectrum," *IEEE Commun. Lett.*, vol. 3, no. 11, pp. 317–319, Nov 1999.

[19] M. Chiani, D. Dardari, and M. K. Simon, "New exponential bounds and approximations for the computation of error probability in fading channels," *IEEE Trans. Wireless Commun.*, vol. 2, no. 4, pp. 840–845, July 2003.

[20] H. Moon and D. Cox, "Improved performance upper bounds for terminated convolutional codes," *IEEE Commun. Lett.*, vol. 11, no. 6, pp. 519–521, June 2007.

[21] N. Kim and H. Park, "Bit error performance of convolutional coded MIMO system with linear MMSE receiver," *IEEE Trans. Wireless Commun.*, vol. 8, no. 7, pp. 3420–3424, July 2009.

[22] Y. Huang and J. Ritcey, "Tight BER bounds for iteratively decoded bit-interleaved space-time coded modulation," *IEEE Commun. Lett.*, vol. 8, no. 3, pp. 153–155, March 2004.

[23] M. McKay and I. Collings, "Capacity and performance of MIMO-BICM with zero-forcing receivers," *IEEE Trans. Commun.*, vol. 53, no. 1, pp. 74–83, Jan 2005.

[24] S. Benedetto and G. Montorsi, "Unveiling turbo codes: some results on parallel concatenated coding schemes," *IEEE Trans. Inf. Theory*, vol. 42, no. 2, pp. 409–428, 1996.

[25] S. Benedetto and G. Montorsi, "Performance evaluation of parallel concatenated codes," in *Proc. IEEE Int. Conf. Commun. (ICC)*, vol. 2, 1995, pp. 663–667 vol.2.

[26] E. Hall and S. Wilson, "Design and analysis of turbo codes on Rayleigh fading channels," *IEEE J. Sel. Areas Commun.*, vol. 16, no. 2, pp. 160–174, 1998.

[27] N. Mysore and J. Bajcsy, "BER bounding techniques for selected turbo coded MIMO systems in Rayleigh fading," in *Proc. 44th Annual Conf. Inf. Sci. Syst. (CISS)*, 2010, pp. 1–6.

[28] K. Keith, *Mathematical Statistics*. USA: CHAPMAN & HALL/CRC, 2000.

[29] A. S. Spiegel Murray, John Schiller and M. LeVan, *Probability and Statistics*. New York, USA: Mcgraw-hill, 2009.

[30] A. Khansefid and H. Minn, "On channel estimation for massive MIMO with pilot contamination," *IEEE Commun. Lett.*, vol. 19, no. 9, pp. 1660–1663, 2015.

[31] H. Xie, F. Gao, and S. Jin, "An overview of low-rank channel estimation for massive MIMO systems," *IEEE Access*, vol. 4, pp. 7313–7321, 2016.

[32] Z. Chen, L. Wang, Z. Zhao, and H. Huang, "ICA filtering based channel estimation for massive MIMO TDD systems," *IEEE Commun. Lett.*, vol. 20, no. 11, pp. 2253–2256, 2016.

[33] C. K. Wen, S. Jin, K. K. Wong, J. C. Chen, and P. Ting, "channel estimation for massive MIMO using Gaussian-mixture Bayesian learning," *IEEE Trans. Wireless Commun.*, vol. 14, no. 3, pp. 1356–1368, 2015.

[34] C. Qi and L. Wu, "Uplink channel estimation for massive MIMO systems exploring joint channel sparsity," *Electron Lett.*, vol. 50, no. 23, pp. 1770–1772, 2014.

[35] G. Stewart, *Matrix Algorithms: Volume 1, Basic Decompositions*, 1st ed. Cambridge University Press, 1998.

[36] A. Al-Askery, C. C. Tsimenidis, S. Boussakta, and J. A. Chambers, "Improved coded massive MIMO OFDM detection using LLRs derived from complex ratio distributions," in *Proc. IEEE 20th Int. Workshop Comput. -Aided Modelling. Design of Commun. Links Netw. (CAMAD)*, Sep. 2015, pp. 64–68.

[37] J. Proakis and M. Salehi, *Digital Communications*, 5th ed. McGraw-Hill, 2008.

[38] M. H. DeGroot, *Probability and Statistics*, 2nd ed. Addison-Wesley, 1989.

[39] M. Ahmed, C. Tsimenidis, and S. Le Goff, "Performance analysis of full-duplex MIMO-SVD-SIC based relay in the presence of channel estimation errors," in *Proc. IEEE 10th Int. Conf. Wireless Mobile Comput. Netw. Commun. (WiMob)*, Oct 2014, pp. 467–472.

[40] I. Gradshteyn and I. Ryzhik, *Table of Integrals, Series, and Products*, 7th ed. Elsevier, 2007.

[41] T. M. Duman and A. Ghrayeb, *Coding for MIMO Communication Systems*. John Wiley & Sons, 2008.

[42] G. L. Stuber, *Principles of Mobile Communication*, 3rd ed. Springer, 2011.

[43] J. Kiusalaas, *Numerical Methods in Engineering with Python*, 2nd ed. Cambridge University Press, 2010.

[44] R. L. Burden and J. D. Faires, *Numerical Analysis*, 9th ed. Brooks/Cole, USA, 2011.

[45] G. H. Golub and C. F. Van Loan, *Matrix Computations*, 3rd ed. JHU Press, 1996.

[46] A. Papoulis and S. U. Pillai, *Probability, Random Variables, and Stochastic Processes*, 3rd ed. McGraw-Hill Education, 1991.

[47] F. G. Alexander McFarlane Mood and D. Boes, *Introduction to the Theory of Statistics*, 3rd ed. McGraw-Hill, 1974.

Ali Al-Askery (S'14)is a Lecturer in the Electrical Engineering Technical College / Middle Technical University, Baghdad, Iraq. He received the B.Sc. and M.Sc. degrees in Electrical Engineering from Al-Mustansiriya University, Baghdad, Iraq, in 2001 and 2004, respectively. He received his PhD from the School of Electrical and Electronics Engineering, Newcastle University, Newcastle Upon Tyne, U.K. His research focuses on wireless communications of MIMO systems, OFDM systems, coded systems and receiver design.

This work is licensed under a Creative Commons Attribution 3.0 License. For more information, see http://creativecommons.org/licenses/by/3.0/.

This article has been accepted for publication in a future issue of this journal, but has not been fully edited. Content may change prior to final publication. Citation information: DOI 10.1109/TCOMM.2017.2749370, IEEE Transactions on Communications

Charalampos C. Tsimenidis is a Senior Lecturer in Signal Processing for Communications in the School of Electrical and Electronic Engineering. He received his PhD in Communications and Signal Processing from Newcastle University in 2002. His main research expertise and interests are in the area of adaptive array receivers for wireless communications including demodulation algorithms, network coding and protocol design for radio frequency and underwater acoustic channels. He has published over 190 conference and journal papers, supervised successfully 3 MPhil and 35 PhD Students and made contributions in the area of arrayed receiver design for doubly-spread multipath fading channels to several UK and European funded research projects. He is a senior member of the IEEE and a member of the IET.

Said Boussakta (S89-M90-SM04) received the Ingenieur dEtat degree in Electronic Engineering from the National Polytechnic Institute of Algiers, Algeria in 1985 and the PhD degree in Electrical Engineering from Newcastle University, U.K., in 1990. From 1990-1996, he was with Newcastle University as a Senior Research Associate in Digital Signal Processing. From 1996-2000, he was with the University of Teesside, UK, as a Senior Lecturer in Communication Engineering. From 2000-2006 he was at the University of Leeds as a Reader in Digital Communications and Signal Processing. He is currently a Professor of Communications and Signal Processing at the School of Electrical and Electronic Engineering, Newcastle University, where he is lecturing in Communication Networks and Signal Processing subjects. His research interests are in the areas of fast DSP algorithms, Digital Communications, Communication Network Systems, Cryptography, and Digital Signal/Image Processing. He has authored and coauthored more than 200 publications and served as Chair for Signal Processing for Communications Symposium in ICC06, ICC07, ICC08, ICC2010 and ICC2013. Prof Boussakta is a Fellow of the IET, and a Senior Member of the Communications and Signal Processing Societies.

J. A. Chambers (S83M90SM98F11) received the Ph.D. and D.Sc. degrees in signal processing from the Imperial College of Science, Technology and Medicine (Imperial College London), London, U.K., in 1990 and 2014, respectively. From 1991 to 1994, he was a Research Scientist with the Schlumberger Cambridge Research Center, Cambridge, U.K. In 1994, he returned to Imperial College London as a Lecturer in signal processing and was promoted to Reader (Associate Professor) in 1998. From 2001 to 2004, he was the Director of the Center for Digital Signal Processing and a Professor of signal processing with the Division of Engineering, Kings College London and is now a Visiting Professor. From 2004 to 2007, he was a Cardiff Professorial Research Fellow with the School of Engineering, Cardiff University, Cardiff, U.K. Between 20072014, he led the Advanced Signal Processing Group, within the School of Electronic, Electrical and Systems Engineering at Loughborough University and is now a Visiting Professor. In 2015, he joined the School of Electrical and Electronic Engineering, from the 1st Aug 2017 the School of Engineering, Newcastle University, where he is a Professor of signal and information processing and heads the Intelligent Sensing and Communications group. He is also an International Honorary Dean and Guest Professor within the Department of Automation at Harbin Engineering University, China. He has advised almost 80 researchers through to Ph.D. graduation and published more than 500 conference proceedings and journal articles, many of which are in IEEE journals. His research interests include adaptive signal processing and machine learning and their application in communications, defence and navigation systems. Dr. Chambers is a Fellow of the Royal Academy of Engineering, U.K., the Institution of Engineering and Technology, and the Institute of Mathematics and its Applications. He was a Technical Program Cochair for the 36th IEEE International Conference on Acoustics, Speech, and Signal Processing (ICASSP), Prague, Czech Republic and is serving on the organising committees of ICASSP 2019 Brighton, UK, and ICASSP 2022, Singapore. He has served on the IEEE Signal Processing Theory and Methods Technical Committee for six years, the IEEE Signal Processing Society Awards Board for three years, and the Jack Kilby Medal Commitee for three yeasr. He has also served as an Associate Editor for the IEEE TRANSACTIONS ON SIGNAL PROCESSING for three terms over the periods 19971999, 20042007, and as a Senior Area Editor 20112015.

This work is licensed under a Creative Commons Attribution 3.0 License. For more information, see http://creativecommons.org/licenses/by/3.0/.